VOL. 12. NO. 1 AUGUST 2026
P-ISSN: 2685-8223 | E-ISSN: 2527-4864
DOI: 10.33480/jitk.v12i1.8446



# PULMONARY EDEMA CLASSIFICATION USING CLASSICAL AND QUANTUM CONVOLUTIONAL NEURAL NETWORKS

**Adri Sopiana[1]; Tony Sumaryada[1]; Sitti Yani[1*]**

Department of Physics, Faculty of Mathematics and Natural Sciences[1]
IPB University, Bogor, Indonesia[1]
https://www.ipb.ac.id/id/[1]
sittiyani@apps.ipb.ac.id[*]

(*) Corresponding Author
(Responsible for the Quality of Paper Content)



***Abstract***— *This study develops a pulmonary edema detection model based on chest x-ray images using both classical Convolutional Neural Network (CNN) and Quantum Convolutional Neural Network (QCNN) approaches. The dataset consists of chest x-ray images labeled as positive and negative for pulmonary edema and is divided into training and testing sets with an 80:20 ratio. To obtain the best performance, both models were optimized through hyperparameter tuning. The classical CNN model employed 3×3 filters, four convolutional layers, and was trained for 10 epochs. The QCNN model was designed with a comparable architecture incorporating quantum gate modifications and was also trained for 10 epochs. The performances of these models were assessed based on accuracy, sensitivity, and precision in order to measure their classification capacities. The QCNN was developed under the same experimental conditions to enable a fair performance comparison with the optimized classical CNN model. The results show that the classical CNN achieved better performance than the QCNN. This lower QCNN performance is likely due to the current limitations of quantum architectures and hardware, which are not yet able to extract and process image features as effectively as classical CNNs. However, this study was conducted using low-resolution medical images and a preliminary QCNN framework under limited computational resources.*

***Keywords***: *CNN, Hyperparameters, Pulmonary Edema, QCNN, X-Ray Image.*

**Intisari**— *Penelitian ini mengembangkan model deteksi edema paru berdasarkan citra rontgen dada menggunakan pendekatan classical Convolutional Neural Network (CNN) dan Quantum Convolutional Neural Network (QCNN). Dataset yang digunakan terdiri atas citra rontgen dada dengan label edema paru positif dan negatif, yang dibagi menjadi data latih dan data uji dengan rasio 80:20. Untuk memperoleh kinerja terbaik, kedua model dioptimasi melalui penalaan hiperparameter. Model CNN klasik menggunakan filter berukuran 3×3, empat lapisan konvolusi, dan dilatih selama 10 epoch. Model QCNN dirancang dengan arsitektur yang sebanding melalui modifikasi gerbang kuantum dan juga dilatih selama 10 epoch. Performa kedua model dievaluasi berdasarkan nilai akurasi, sensitivitas, dan presisi untuk mengukur kemampuan klasifikasinya. QCNN dibangun dalam kondisi eksperimental yang sama untuk memungkinkan perbandingan kinerja yang adil dengan model CNN klasik yang telah dioptimasi. Hasil penelitian menunjukkan bahwa CNN klasik memberikan kinerja yang lebih baik dibandingkan QCNN. Kinerja QCNN yang lebih rendah diduga disebabkan oleh keterbatasan arsitektur dan perangkat keras kuantum saat ini, yang belum mampu mengekstraksi dan memproses fitur citra seefisien CNN klasik. Namun, penelitian ini dilakukan menggunakan citra medis beresolusi rendah dan implementasi QCNN awal dengan keterbatasan sumber daya komputasi.*

***Kata Kunci***: *CNN, Hiperparameter, Edema Paru, QCNN, Citra Sinar-X.*



Accredited Rank 2 (Sinta 2) based on the Decree of the Dirjen Penguatan RisBang Kemenristekdikti No.225/E/KPT/2022, December 07, 2022. Published by LPPM Universitas Nusa Mandiri

VOL. 12. NO. 1 AUGUST 2026
P-ISSN: 2685-8223 | E-ISSN: 2527-4864
DOI: 10.33480/jitk.v12i1.8446

## INTRODUCTION

The chest or thorax is one of the most important parts of the human body. It houses vital organs that are essential for human survival, such as the circulatory, digestive, and respiratory systems. Other organs throughout the body cannot function properly and experience a decline in function when these vital organs are diseased or malfunctioning. Various diseases can affect the respiratory system, especially the lungs, such as tuberculosis, edema, pneumonia, bronchitis, and others [1].

Acute pulmonary edema is a medical emergency that requires immediate and appropriate management, characterized by swelling of the lungs due to fluid buildup in the air sacs (alveoli) and lung tissue. Acute pulmonary edema is characterized by symptoms including severe shortness of breath and hypoxia caused by fluid buildup in the lungs, which disrupts gas exchange and causes lung collapse [2]. The annual mortality rate for patients hospitalized with acute pulmonary edema reaches 40%. The most common causes of acute pulmonary edema include myocardial ischemia, cardiac arrhythmia (e.g., atrial fibrillation), heart valve dysfunction, and fluid overload. In addition, it can also be caused by other factors, including pulmonary embolism, renal artery stenosis, non-compliance with treatment for previous illnesses, and side effects from certain medications [3], [4].

The diagnosis of pulmonary edema is made through a combination of clinical evaluation, physical examination, blood gas analysis, and radiological examination, particularly chest x-rays. On x-ray images, pulmonary edema is generally characterized by the presence of bilateral diffuse infiltrates, increased vascular shadowing, and a distinctive appearance such as a “batwing” pattern [2], [5], [6]. However, the interpretation of x-ray images is highly dependent on the experience and expertise of the radiologist, which opens up the possibility of misdiagnosis or delays in medical decision-making [7], [8].

To overcome these challenges, machine learning (ML) has begun to be widely applied in the medical world, particularly in detecting and analyzing radiological images especially pulmonary edema with relatively simpler image complexity. ML enables computer systems to learn from existing data and make decisions automatically [9], [10]. One of the most commonly used ML methods in medical image processing is Convolutional Neural Network (CNN), which is designed to recognize patterns in images accurately and efficiently. In this context, ML is not intended to replace the role of radiologists, but rather as a tool or second opinion that can strengthen x-ray image-based diagnosis results [11], [12], [13]. Previous studies have shown that deep learning approaches, particularly CNNs, can be used to detect and classify pulmonary edema in chest X-ray images [14], [15], [16].

Currently, Quantum Convolutional Neural Network (QCNN) has emerged as a development of CNN using quantum concepts, where the combination of CNN and Quantum Computing has the potential to perform faster and more specific training [17], [18]. The application of QCNN to cases of pulmonary edema is still relatively limited; therefore, this study uses pulmonary edema as the classification target .While standard CNNs depend wholly on traditional computations, QCNNs employ quantum computing techniques like superposition and entanglement to perform calculations in quantum feature space. This has the ability to offer advantages in terms of having smaller model representations and efficiency in computation for specific machine learning problems. Nevertheless, the use of QCNNs in classifying medical images is still fairly new, especially in experiments where there is direct comparison between QCNNs and traditional CNN models in light resource conditions. Hence, comparison of QCNN and a standard lightweight CNN would be critical in gauging the viability of quantum image classifiers in medical imaging.

Therefore, this study designed an ML model that can strengthen the detection results of pulmonary edema from x-ray images for the classification of edema and non-edema diseases and calculate the accuracy obtained from classic and quantum CNN models for the classification of x-ray images in detecting pulmonary edema.

## MATERIALS AND METHODS

### Dataset

The dataset used in this study consists of two classes, namely Edema and NoEdema with 1024×1024 pixels (Figure 1). This dataset was taken from kaggle.com, after which a directory was created on Google Drive to prepare for data retrieval. The preprocessing stage involved resizing the images to a resolution of 16×16 pixels for CNN and QCNN to improve computational efficiency and enable lightweight classification experiments under limited computational resources. Similar lightweight medical imaging benchmarks, such as MedMNIST, also employ low-resolution images for rapid prototyping and classification studies [19]. Although low-resolution preprocessing may reduce fine anatomical details, this study was limited to image-level classification rather than lesion localization or segmentation. Each image was read in color format and resized using the resize method from OpenCV. The dataset was then converted into a numeric array using NumPy for further processing in the model. The complete dataset used in this study consisted of 4000 images. However, variations in dataset size were intentionally applied during the experiments to investigate the effect of training data quantity on the performance of the CNN and QCNN models.

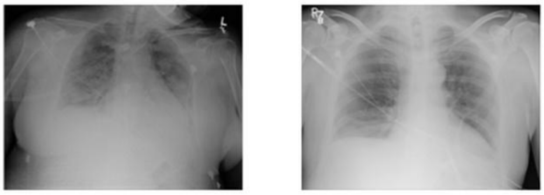

(a) (b)

Source: (Bari [21], 2023)

Figure 1. X-Ray Image of (a) Edema and (b) no-Edema

**Preprocessing data**

The data that has been converted into a numeric array will be split into training data and test data using the train_test_split function from sklearn, with a composition of 80% for training data and 20% for test data. The dataset consists of 2000 Edema images and 2000 no Edema images. Since the dataset is balanced, there is no imbalance issue in the data classes and oversampling is not necessary.

**CNN Architecture**

Convolutional neural networks (CNN) models are used to perform classification on x-ray image datasets. In this model, convolution layers defined as Conv classes are used. The following is the CNN layer architecture:

1. Conv2D: 3×3 kernel with 'same' padding and ReLU activation.
2. BatchNormalization: Placed after convolution to stabilize training.
3. Fully Connected Layer: Dense(16, ReLU), Dense(1, sigmoid).

In the last fully connected layer, the sigmoid activation layer function is used in the output to predict the probability of a binary class, namely edema or no edema. The CNN architecture in this study was designed simply, with a single convolutional layer, Batch Normalization, and two fully connected layers to keep the model's complexity low and accommodate computational constraints. This lightweight approach was also adopted to ensure a more balanced comparison with the QCNN model under identical experimental conditions. The primary focus of this study is not on developing complex deep learning architectures, but rather on an initial evaluation of the performance and efficiency of the QCNN approach for x-ray image classification.

**QCNN Architecture**

Quantum Convolutional Neural Networks (QCNN) models were developed to perform classification on X-ray image datasets. In this model, a special quantum convolution layer defined as the QConv class is used. This layer utilizes qubits arranged in a grid, where each qubit represents one pixel of the input image. The convolution process is performed using two types of quantum gates, namely the Hadamard quantum gate and the z-axis rotation (RZ) gate, which are applied to pairs of qubits. Each quantum operation contains learning parameters that are optimized during the model training process. This quantum layer is then followed by several additional layers, including: flatten layer to convert the quantum convolution data into a 1D vector form, fully connected layer (dense layer) to perform classification on x-ray image data, and sigmoid activation layer is used at the output to predict the probability of a binary class, namely edema or no edema.

This proposed QCNN architecture incorporates 4 qubits, employing the angle encoding technique for expressing image data as quantum states. Quantum convolution is carried out via Hadamard gates and rotations along the Z axis (RZ gates) as parametrized quantum circuits, while entanglement of the qubits is done using the CNOT and CZ gates. The quantum circuit architecture involves a shallow design that comprises a single quantum convolutional layer.

**Model training**

The model was trained using the Adam optimizer with the binary_crossentropy loss function, as this research is a binary classification problem. The model was trained for 10 epochs. In addition, the accuracy metric was used to measure the model's performance during training. To avoid overfitting and optimize performance, a validation process was carried out using test data.

**Model evaluation**

The evaluation process is carried out by measuring accuracy and displaying a classification report that includes sensitivity (recall) and precision values, using a confusion matrix. A confusion matrix is a matrix used to describe and assess the performance of a classification model. The confusion matrix consists of True Positive (TP),


Accredited Rank 2 (Sinta 2) based on the Decree of the Dirjen Penguatan RisBang Kemenristekdikti No.225/E/KPT/2022, December 07, 2022. Published by LPPM Universitas Nusa Mandiri

VOL. 12. NO. 1 AUGUST 2026
P-ISSN: 2685-8223 | E-ISSN: 2527-4864
DOI: 10.33480/jitk.v12i1.8446

False Positive (FP), True Negative (TN), and False Negative (FN). The confusion matrix can be used to determine accuracy, sensitivity, precision, and f1-score. Accuracy is the ratio of true positive and true negative predictions to all data, precision is the ratio of true positives to positive predictions, sensitivity (recall) is the ratio of true positive predictions to all actual positive data, and f1-score is a combination of sensitivity and precision that provides a balanced value between them (Equation (1)-(4)). These three evaluation values are used to assess the effectiveness of the model in detecting edema images.

$$\text{Accuracy} = \frac{TP+TN}{TP+TN+FP+FN} \quad (1)$$

$$\text{Precision} = \frac{TP}{TP+FP} \quad (2)$$

$$Recall = \frac{TP}{TP+FN} \quad (3)$$

$$f1\text{-}score = 2\,\frac{Recall \times Precision}{Recall+Precision} \quad (4)$$

## RESULTS AND DISCUSSION

### Data handling

This study uses an x-ray image dataset obtained from the Kaggle platform, with categories of no edema and edema, each consisting of 500 images, for a total of 1,000 images. This dataset was uploaded by Pulmonary Edema Classified - by NIH [21]. The number of datasets was then increased to 2000 and then 3000 images to explore the effect of the number of datasets on model performance. Additional datasets were taken from the Kaggle page uploaded by Mooney (2018) for normal data (Chest X-ray Images (Pneumonia)) and edema image data from Shedge's (2024) upload (Chest Xray). Then the dataset was added again to 4000 images. The additional dataset for a total of 4000 images was taken from the Kaggle page uploaded by Vaitheeswaran (2024) (pulmonary-edema). From each variation in the number of datasets, it was divided into two parts: 80% as training data and 20% as test data (Table 1).

Table 1. Data splitting (source: author's own work)

| No | Category | Number of data | | | | | | | |
|---|---|---|---|---|---|---|---|---|---|
| | | 1000 | | 2000 | | 3000 | | 4000 | |
| | | Tr* | Te* | Tr* | Te* | Tr* | Te* | Tr* | Te* |
| 1 | No edema | 400 | 100 | 800 | 200 | 1200 | 300 | 1600 | 400 |
| 2 | Edema | 400 | 100 | 800 | 200 | 1200 | 300 | 1600 | 400 |
| | Total | 800 | 200 | 1600 | 400 | 2400 | 600 | 3200 | 800 |

Source: [21]
*Tr= training
** Te = test

The variation in the amount of data added refers another study which used data variations of 1000, 10000, and 100000. An increase in the amount of data improved accuracy but not significantly, only by about 2%. However, in this study, the data used varied from 1000, 2000, 3000, and 4000 images due to data source limitations. This was possible due to patient privacy, a lack of cases due to rare conditions, and organizational and legal challenges [22]. In this study, the dataset used consists of a number of color images in RGB (Red, Green, Blue) format.

All images were converted to grayscale format to simplify the processing stage. This was done because grayscale images only have one channel that represents light intensity, unlike RGB images, which have three color channels (red, green, and blue) that are more complex to process [23]. Each grayscale image initially has dimensions of 1024×1024 pixels, but is then resized to 16×16 pixels (Figure 1). The purpose of this resolution reduction is to speed up the model training process. Although the images appear slightly blurry after being reduced in size, the model can still recognize important information in the images.

Previous research by Khanday et al. (2021) shows that the use of small images not only speeds up training, but can also improve model accuracy compared to the use of large images [24]. After the image size is reduced, the image data is then converted into a matrix form to facilitate the model training process. Each image is converted into a matrix using the NumPy library, so that each pixel has its own gray intensity value. This step is important because CNN algorithms and other Machine Learning (ML) techniques generally process data in matrix format [25].

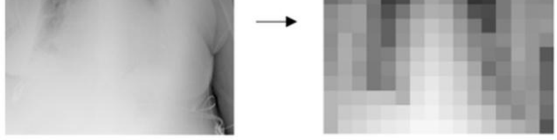

Source: (Bari [21], 2023)
Figure 2. Image Resizing

VOL. 12. NO. 1 AUGUST 2026
P-ISSN: 2685-8223 | E-ISSN: 2527-4864
DOI: 10.33480/jitk.v12i1.8446



**CNN model implementation**

The CNN model was designed with an architecture consisting of one convolutional layer with a 3×3 kernel, followed by one Batch Normalization layer and two fully connected Dense layers. One technique implemented to improve the performance of the CNN model was Batch Normalization. This technique was inserted after the convolutional layer and before the activation function in the network architecture. The use of Batch Normalization helps stabilize the distribution of values between layers, accelerate convergence, and improve model generalization. This normalization mechanism works by standardizing the output from the previous layer based on the mean and standard deviation of the mini-batch, thereby reducing internal distribution shifts (internal covariate shift). The model not only learns faster but is also more robust to changes in input scale and initial weight variations. The model then ends with a Fully Connected Layer with 16 units and a ReLU activation function, equipped with one output neuron with sigmoid activation, suitable for binary classification between the Edema and No Edema classes. After that, the model is compiled using the Adam optimizer, the binary_crossentropy loss function, and the accuracy metric. At the model training stage, a batch size of 32 and 10 epochs are used.

The experiment was conducted with datasets consisting of 1000, 2000, 3000, and 4000 images. With a dataset of 1000 images, the CNN model produced an accuracy of 71.50% (Figure 3). When the dataset size was increased to 2000, the model accuracy increased to 85.50%. This approach is in line with common practice in deep learning model development, where initial experiments are conducted using medium-sized datasets to evaluate the effectiveness and feasibility of the model architecture before it is optimized and applied to larger and more complex datasets. Therefore, a dataset consisting of 3000 images was selected for the training and evaluation of the CNN model described in the next section.

When the data was increased to 3000, the accuracy increased significantly to 91.33%. This increase shows that the CNN model is very responsive to additional data. However, when the amount of data was increased to 4000, the increase in accuracy was not very significant, reaching only 91.13% (Figure 3), indicating a saturation point in performance as the amount of data increases, in line with the phenomenon of diminishing returns in machine learning [26].

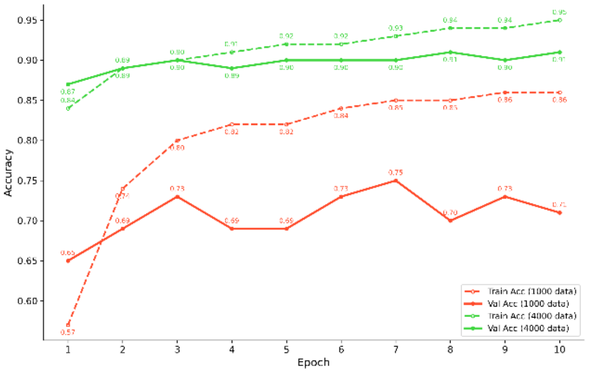


Source: (Research Results, 2026)
Figure 3. Comparison of CNN Accuracy on 1000 Images and 4000 Images

Figure 3 shows that the CNN model is capable of yielding an accuracy of 91.33%. The high performance of CNN indicates a good balance between classes. The model does not focus on a particular class, but is able to recognize both classes (no edema and Edema) proportionally. This balance is important, especially in medical classification, because misclassification in one class can have serious implications for patient diagnosis [27].

The model also shows stability during training, as indicated by the accuracy curve, which does not experience sharp fluctuations or signs of overfitting. One factor contributing to this stability is the application of the Batch Normalization technique. Batch Normalization helps stabilize and accelerate network training by normalizing the activation of each mini-batch [28].

**QCNN model implementation**

The design of QCNN model has an architecture with one quantum convolution layer, where features are extracted from input data using quantum gate-based unitary operations. Then, the same Batch Normalization layer is added to the classic CNN. This model ends with a Fully Connected Layer (dense) that combines the extracted features and uses a sigmoid activation function in the output layer to accommodate binary classification problems, so that the output is in the range [0, 1]. This model is compiled using the Adam optimizer, which is known for its stability and efficiency in parameter convergence.

The binary_crossentropy loss function is suitable for binary classification tasks, and the evaluation metric uses accuracy as the main measure of the model's performance in correctly classifying data. The variations made in this QCNN are the application of several different quantum gates and variations in the amount of data.



Accredited Rank 2 (Sinta 2) based on the Decree of the Dirjen Penguatan RisBang Kemenristekdikti No.225/E/KPT/2022, December 07, 2022. Published by LPPM Universitas Nusa Mandiri

JITK (JURNAL ILMU PENGETAHUAN DAN TEKNOLOGI KOMPUTER)
VOL. 12. NO. 1 AUGUST 2026
P-ISSN: 2685-8223 | E-ISSN: 2527-4864
DOI: 10.33480/jitk.v12i1.8446

**Quantum Logic Gate Variations**

Several quantum logic gates are applied as key components in building quantum circuits in QCNN and finding matches to obtain significant accuracy. These gates play a role equivalent to mathematical operations in classical CNNs (such as convolution or activation), but work based on quantum principles. The quantum gates used are CNOT, CZ, Hadamard, and RZ. The Controlled-NOT (CNOT) quantum gate is a two-qubit gate that flips the target qubit if and only if the control qubit is 1. It is used to create entanglement between two qubits, which enables the transfer and correlation of complex information in a network. The reason for using this quantum gate is that entanglement is very important in quantum computing because it enables non-classical correlations that cannot be replicated by classical CNN. The Controlled-Z (CZ) gate is a two-qubit gate that applies a π-phase shift to the target qubit only if the control qubit is in the $|1\rangle$ state. This gate serves to create phase changes as part of quantum manipulation of information. The reason for using this gate is that CZ works well with CNOT in building complex circuits and can enrich the representation of information in data features [29].

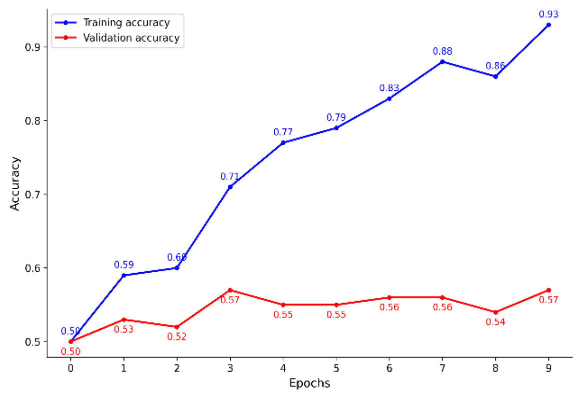


Source: (Research Results, 2026)
Figure 4. Accuracy of QCNN using CNOT and CZ Quantum Gates

Hadamard is a single-qubit gate that changes the computational basis states $|0\rangle$ and $|1\rangle$ into superposition. It functions to enable qubits to be in a mixed state (superposition), thereby facilitating parallel quantum processing. The reason for using the Hadamard gate is to build circuits with the ability to explore quantum solution spaces. The RZ is a rotation operation on the Z axis in the Bloch sphere by a certain angle θ. It serves to adjust the learning parameter (θ) in the QCNN model. Each rotation parameter can be optimized during the training process. This gate is used because it is flexible as part of model parameterization, while also being efficient in its implementation in simulated quantum circuits.

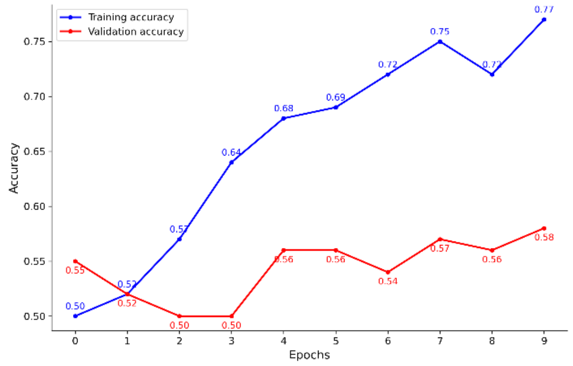


Source: (Research Results, 2026)
Figure 5. Accuracy of QCNN using Hadamard and RZ Quantum Gates

When using Controlled-NOT (CX) and Controlled-Z (CZ) quantum logic gates, the model was tested on test data with a sample size of 200 and obtained a validation accuracy of 57.5% (Figure 4). Then the model was tested using the Hadamard (H) and RZ quantum gates, based on the model prediction, it had a validation accuracy of 58.5% (Figure 5). The implementation of the H and RZ quantum gates in the Quantum Convolutional Neural Network (QCNN) architecture showed better performance than the use of the CX and CZ gates. This was reflected in the increased accuracy of the model in classifying pulmonary edema x-ray images, where the combination of H and rz produced higher accuracy.

The Hadamard gate has the ability to transform the computational basis state into a superposition, allowing qubits to exist in a linear combination of the basis states $|0\rangle$ and $|1\rangle$. This property enables the exploration of a broader solution space, increasing the model's representation capacity in extracting features from input data. Meanwhile, the RZ gate allows the rotation of qubit states around the Z axis on the Bloch sphere by a certain angle, providing flexibility in parameter adjustment during the training process.

The combination of H and RZ allows the model to build feature representations that are more complex and adaptive to data variations. Conversely, the CX and CZ gates function as two-qubit gates that create entanglement between qubits, which is important in quantum information processing. However, in the context of image classification, the use of these gates can introduce additional complexity that does not always contribute positively to model performance. A study by Hirai (2024) shows that the use of CZ gates in

Quantum Neural Network (QNN) models can reduce model expressiveness, especially when the observation axis is set on the Z axis, because phase inversion by CZ gates does not contribute significantly in this context [30]. Therefore, the selection of quantum gates in QCNN architecture must be tailored to the characteristics of the data and the classification objectives. In this case, the combination of Hadamard and RZ gates provides a balance between model complexity and generalization capabilities, resulting in better performance in the classification of pulmonary edema x-ray images.

**Number of Data Variations**

The amount of data used in the QCNN training process greatly affects the model's performance. The initial model was trained with a dataset of 1000 images, but the accuracy obtained was still relatively low. This prompted the gradual addition of data as part of an exploration strategy to find the optimum accuracy point. Several machine learning studies use large and even comprehensive (combined) data sets. The ultimate goal is to find the amount of data that provides a balance between computational load and model performance (modeling efficiency). In addition, an analysis is also carried out to determine whether, after a certain point, adding more data does not provide a significant increase in accuracy.

The initial data set of 1000 images produced an accuracy of around 57.5% and 58.5% (Figures 4 and 5), indicating that the small amount of data made it difficult for the model to recognize patterns. With an accuracy of 58.5% on 1000 images, the next step was to use 2000 images. With 400 test images, the model achieved an accuracy of 73.75%. This accuracy is 15.25% higher than the previous dataset. This explains that the number of datasets greatly affects ML models. Other ML models use a lot of data, even tens and hundreds of thousands of datasets. This variation in the number of datasets is important because, in addition to affecting the model, it must also be balanced with computing power.

The next data variation was 3000 images, considering the computational load and accuracy improvement for the next stage. The selection of 3000 data also considered training time efficiency, model stability, and representation balance between the two classes (Normal and Edema). Additionally, the quantum-based QCNN model requires a sufficient amount of data to extract spatial features optimally. The model was tested on a test dataset of 600 samples. After running, an accuracy of 75.16% was obtained. To increase the data size to 4000 images, edema data was added to the dataset. The data was taken from the Kaggle page uploaded by Vaitheeswaran (2024). After the data was added, the accuracy did not increase but remained at around 75.12%, and when run again, the resulting accuracy was lower.

A significant improvement in the performance of the QCNN model was observed when the data was increased from 1000 to 2000 images. The model's accuracy increased from 58.5% to 73.75%. The highest accuracy was achieved when the dataset consisted of 3000 images. This shows that QCNN is able to utilize the increase in data to better recognize patterns in x-ray edema images. This is supported by other research conducted by Lee et al. (2025), which states that Machine Learning models tend to experience an increase in performance as the size of the training data increases because the model can learn more data feature distributions [26].

However, when the amount of data was increased to 4000, the expected increase in accuracy did not occur. The model's accuracy actually decreased to 75.12%, and could even be lower if the training process was repeated. This indicates a saturation point or diminishing returns, where adding data no longer provides a significant improvement in performance. Another possibility is that the data added in the fourth stage was not sufficiently varied in terms of pattern distribution, or even contained similarities to the previous data already in the training, so it did not add any new information that was useful for the model.

Both models demonstrate the values of sensitivity and precision that show the similar tendency corresponding to accuracy. Thus, with increasing the number of samples in the dataset from 300 to 3,000, both the classical convolutional neural network and the quantum convolutional neural network showed a higher level of sensitivity and precision. This fact means that the ability of these two models to recognize the positive class improved. In the case of the classical model, the sensitivity and precision rose to 0.99, whereas in the case of the quantum one, the maximums reached the values of 0.98–0.99. It is necessary to note that it is caused by the fact that a larger dataset allowed obtaining more information and learning better due to more data variety. Nevertheless, the dataset with the number of 4000 showed the decrease in sensitivity and precision in the case of the H–RZ model, which is a feature similar to that one found in relation to the accuracy in the same case. This phenomenon is caused by the impact of training instability and the inability to represent the data adequately due to its complexity.

VOL. 12. NO. 1 AUGUST 2026
P-ISSN: 2685-8223 | E-ISSN: 2527-4864
DOI: 10.33480/jitk.v12i1.8446

CNN is a highly effective and efficient approach in handling lung X-ray image classification problems for edema detection. CNN is capable of generalizing patterns well and providing accurate classification results with an accuracy of 91.33% for a dataset of 3000 images. This finding reinforces the understanding that CNN, as a deep learning method that has been widely used in medical imaging, remains the preferred choice for image classification research in clinical applications. However, QCNN can also be used because with an accuracy of 75.16%, it demonstrates the effectiveness of QCNN in identifying patterns of pulmonary edema disease images. This implementation has the potential to improve efficiency in the classification process of pulmonary edema severity with fairly good accuracy, contributing significantly to the development of object recognition systems in the field of digital image processing.

The process of simulating pulmonary edema diagnosis based on x-ray images can be carried out more quickly and efficiently with the support of classification models such as CNN and QCNN. The CNN model, which achieves an accuracy of up to 91.33%, is capable of providing accurate classification results, so it can be used as a second opinion to support the decisions of radiologists. In this context, the results obtained can be adjusted or validated with the classification results from the ML model, which can speed up medical decision-making.

The difference in accuracy between CNN and QCNN reflects the level of maturity and stability of the CNN architecture compared to QCNN, which is still in the exploration and simulation stage. One of the main causes of the low accuracy of QCNN is the limitations of the current quantum computing environment. In this study, QCNN was run on classical devices rather than on actual quantum computers, causing the quantum computation process to lose the efficiency and processing scale expected from actual quantum systems [31]. In addition, quantum algorithms are very sensitive to noise and parameter fluctuations, especially in quantum gate and circuit settings, which can hinder the optimal learning process [32]. The QCNN model demonstrated approximately three times shorter training time compared with the CNN model under the same experimental conditions.

However, QCNN still shows potential in medical image classification, especially with a significant increase in accuracy from 57.50% to 75.16% when the dataset is expanded. Research by Henderson et al. (2020) shows that quantum architectures have the potential to outperform classical models in certain tasks, especially as quantum computing advances further. With further development and access to real quantum devices, QCNN is expected to become a competitive alternative for medical image processing in the future [20].

## CONCLUSION

The results of this study demonstrate that chest x-ray images can be effectively classified using machine learning approaches, thereby supporting a more accurate and efficient diagnostic process for pulmonary edema. Based on the testing results, the developed classical CNN model achieved superior performance, with an average accuracy of 91.33%, compared with 75.16% for the QCNN model. These findings indicate that, although QCNN shows potential for classifying pulmonary edema from chest x-ray images, its performance remains lower than that of the classical CNN. Therefore, at the current stage of development, classical CNN remains the more reliable approach for this task. Nevertheless, this study was limited by the use of low-resolution images and the absence of comprehensive validation on real quantum hardware and multi-dataset variability analysis. Future studies may explore higher-resolution medical images and implementation on real quantum hardware platforms to further evaluate the robustness and practical applicability of the proposed approach.

## REFERENCES

[1] F. Campos-Rodríguez *et al.*, “Respiratory Pathology and Cardiovascular Diseases: A Scoping Review,” *Open Respir. Arch.*, vol. 7, no. 1, p. 100392, Jan. 2025, doi: 10.1016/j.opresp.2024.100392.

[2] C. Zanza *et al.*, “Cardiogenic Pulmonary Edema in Emergency Medicine,” *Adv. Respir. Med.*, vol. 91, no. 5, pp. 445–463, Oct. 2023, doi: 10.3390/arm91050034.

[3] W. Abbasi, A. Shahzadi, and A. Aljohani, "Enhanced detection of pulmonary edema in chest X-rays using deep learning ensembles with attention mechanism," J. Digit. Imaging. Inform. Med., vol. 39, no. 4, pp. 2876–2889, Aug. 2026, doi: 10.1007/s10278-025-01710-4.

[4] D. Schulz et al., "A deep learning model enables accurate prediction and quantification of pulmonary edema from chest X-rays," Crit. Care, vol. 27, no. 1, art. no.

201, Dec. 2023, doi: 10.1186/s13054-023-04426-5.

[5] V. V. Danilov, A. O. Makoveev, A. Proutski, I. Ryndova, A. Karpovsky, and Y. Gankin, "Explainable AI to identify radiographic features of pulmonary edema," Radiol. Adv., vol. 1, no. 1, Art. no. umae003, May 2024, doi: 10.1093/radadv/umae003.

[6] J. Kim, M. Hassan, L. Bijulisingh, and M. Paneru, "Atypical Presentation of Cardiogenic Pulmonary Edema: Multiple Subsolid Lung Nodules," *Am. J. Respir. Crit. Care Med.*, vol. 211, no. Abstracts, pp. A2195–A2195, May 2025, doi: 10.1164/ajrccm.2025.211.Abstracts.A2195.

[7] H. M. S. S. Herath, H. M. K. K. M. B. Herath, N. Madusanka, and B.-I. Lee, "A Systematic Review of Medical Image Quality Assessment," *J. Imaging*, vol. 11, no. 4, p. 100, Apr. 2025, doi: 10.3390/jimaging11040100.

[8] H. Matsuo *et al.*, "Artificial intelligence for chest radiography: an overview of techniques, challenges, and future directions," *Npj Health Syst.*, vol. 3, no. 1, p. 41, Jun. 2026, doi: 10.1038/s44401-026-00087-y.

[9] E. Yuliawan and Shofwatul 'Uyun, "Chest X-ray Image Classification for COVID-19 diagnoses," *J. Inf. Syst. Eng. Bus. Intell.*, vol. 8, no. 2, pp. 109–118, Oct. 2022, doi: 10.20473/jisebi.8.2.109-118.

[10] A. Sinra and H. Angriani, "Automated Classification of COVID-19 Chest X-ray Images Using Ensemble Machine Learning Methods," *Indones. J. Data Sci.*, vol. 5, no. 1, pp. 45–53, Mar. 2024, doi: 10.56705/ijodas.v5i1.127.

[11] Y. Pamungkas, M. R. N. Ramadani, and E. N. Njoto, "Effectiveness of CNN Architectures and SMOTE to Overcome Imbalanced X-Ray Data in Childhood Pneumonia Detection | Journal of Robotics and Control (JRC)," May 2024, Accessed: Oct. 25, 2025. [Online]. Available: https://journal.umy.ac.id/index.php/jrc/article/view/21494

[12] C.-T. Yen and C.-Y. Tsao, "Lightweight convolutional neural network for chest X-ray images classification," *Sci. Rep.*, vol. 14, no. 1, p. 29759, Nov. 2024, doi: 10.1038/s41598-024-80826-z.

[13] M. A. Anwar, Y. A. Gerhana, and U. Syaripudin, "Implementasi Model CNN ResNet50V2 untuk Klasifikasi Pneumonia pada Citra X-Ray," *SMATIKA J. STIKI Inform. J.*, vol. 15, no. 01, pp. 126–135, Jun. 2025, doi: 10.32664/smatika.v15i01.1538.

[14] T. Huang, R. Yang, L. Shen, A. Feng, L. Li, N. He, S. Li, L. Huang, and J. Lyu, "Deep transfer learning to quantify pleural effusion severity in chest X-rays," BMC Med. Imaging, vol. 22, art. no. 100, May 2022, doi: 10.1186/s12880-022-00827-0.

[15] L. Liong-Rung *et al.*, "Using Artificial Intelligence to Establish Chest X-Ray Image Recognition Model to Assist Crucial Diagnosis in Elder Patients With Dyspnea," *Front. Med.*, vol. 9, p. 893208, Jun. 2022, doi: 10.3389/fmed.2022.893208.

[16] "Pulmonary Edema and Pleural Effusion Detection Using EfficientNet-V1-B4 Architecture and AdamW Optimizer from Chest X-Rays Images," *Comput. Mater. Contin.*, vol. 80, no. 1, pp. 1055–1073, Jul. 2024, doi: 10.32604/cmc.2024.051420.

[17] D. Bokhan, A. S. Mastiukova, A. S. Boev, D. N. Trubnikov, and A. K. Fedorov, "Multiclass classification using quantum convolutional neural networks with hybrid quantum-classical learning," *Front. Phys.*, vol. 10, p. 1069985, Nov. 2022, doi: 10.3389/fphy.2022.1069985.

[18] R. Giuntini, F. Holik, D. K. Park, H. Freytes, C. Blank, and G. Sergioli, "Quantum-inspired algorithm for direct multi-class classification," *Appl. Soft Comput.*, vol. 134, p. 109956, Feb. 2023, doi: 10.1016/j.asoc.2022.109956.

[19] J. Yang *et al.*, "MedMNIST v2 - A large-scale lightweight benchmark for 2D and 3D biomedical image classification," *Sci. Data*, vol. 10, no. 1, p. 41, Jan. 2023, doi: 10.1038/s41597-022-01721-8.

[20] M. Yousif, B. Al-Khateeb, and B. Garcia-Zapirain, "A New Quantum Circuits of Quantum Convolutional Neural Network for X-Ray Images Classification," IEEE Access, vol. 12, pp. 61973–61990, May 2024, doi: 10.1109/ACCESS.2024.3396411.

[21] "Pulmonary Edema Classified - By NIH." Accessed: Oct. 25, 2025. [Online]. Available: https://www.kaggle.com/datasets/samiulbari/pulmonary-edema-classified-by-nih

[22] J. Guan, "Fundamental Overview of Medical Scientific Data Sharing," in Governance and Management of Medical Scientific Data Sharing and Application, Singapore: Springer, 2026, pp. 1–35, doi: 10.1007/978-981-95-2806-6_1.

[23] A. S, S. Kashyap, D. Patel H N, and P. Kumar Y R, "Hybrid deep learning and machine learning framework for automated pneumonia detection in chest X-ray images,"

VOL. 12. NO. 1 AUGUST 2026
P-ISSN: 2685-8223 | E-ISSN: 2527-4864
DOI: 10.33480/jitk.v12i1.8446

*MethodsX*, vol. 15, p. 103729, Dec. 2025, doi: 10.1016/j.mex.2025.103729.

[24] S. Dwijayanti et al., "Facial recognition and body temperature measurements based on thermal images using a deep-learning algorithm," IAES Int. J. Artif. Intell. (IJ-AI), vol. 12, no. 4, pp. 1654–1665, Dec. 2023, doi: 10.11591/ijai.v12.i4.pp1654-1665.

[25] K. Y. Cheng, M. Lange-Hegermann, J.-B. Hövener, and B. Schreiweis, "Instance-level medical image classification for text-based retrieval in a medical data integration center," *Comput. Struct. Biotechnol. J.*, vol. 24, pp. 434–450, Jun. 2024, doi: 10.1016/j.csbj.2024.06.006.

[26] J. Lee, H. Chung, M. Suh, J.-H. Lee, and K. S. Choi, "Deep learning for deep learning performance: How much data is needed for segmentation in biomedical imaging?," *PLOS ONE*, vol. 20, no. 12, p. e0339064, Des 2025, doi: 10.1371/journal.pone.0339064.

[27] J. Hofmeister et al., "Validating the accuracy of deep learning for the diagnosis of pneumonia on chest x-ray against a robust multimodal reference diagnosis: a post hoc analysis of two prospective studies," *Eur. Radiol. Exp.*, vol. 8, no. 1, art. no. 20, Feb. 2024, doi: 10.1186/s41747-023-00416-y.

[28] I. D. Mienye, T. G. Swart, G. Obaido, M. Jordan, and P. Ilono, "Deep Convolutional Neural Networks in Medical Image Analysis: A Review," *Information*, vol. 16, no. 3, p. 195, Mar. 2025, doi: 10.3390/info16030195.

[29] Y. Liu, K. Kaneko, K. Baba, J. Koyama, K. Kimura, and N. Takeda, "Analysis of Parameterized Quantum Circuits: On the Connection Between Expressibility and Types of Quantum Gates," *IEEE Trans. Quantum Eng.*, vol. 6, pp. 1–12, 2025, doi: 10.1109/TQE.2025.3571484.

[30] H. Hirai, "Practical application of quantum neural network to materials informatics," *Sci. Rep.*, vol. 14, no. 1, p. 8583, Apr. 2024, doi: 10.1038/s41598-024-59276-0.

[31] A. Cicero, M. A. Maleki, M. W. Azhar, A. F. Kockum, and P. Trancoso, "Simulation of Quantum Computers: Review and Acceleration Opportunities," *ACM Trans. Quantum Comput.*, vol. 7, no. 1, p. 3:1-3:35, Nov. 2025, doi: 10.1145/3762672.

[32] M. C. Caro, H.-Y. Huang, M. Cerezo, K. Sharma, A. Sornborger, L. Cincio, and P. J. Coles, "Generalization in quantum machine learning from few training data," Nat. Commun., vol. 13, no. 1, art. no. 4919, Aug. 2022, doi: 10.1038/s41467-022-32550-3.